

where

$$\begin{aligned}
 S_A &= (n/2)[M_1(1 + b_{66}^*/a^*) + 2d_{66}^*/a^*]p_n \\
 S_B &= (n/2)[M_2(1 + b_{66}^*/a^*) + 2d_{66}^*/a^*]q_n \\
 S_C &= -M_1 n^2/4 \quad S_D = -M_2 n^2/4 \\
 S_E &= p_n^3(b_{12}^*M_1 - d_{11}^*) + (p_n/4)[d_{12}^* + 4d_{66}^* - \\
 &\quad M_1(b_{11}^* - 2b_{66}^*)]n^2 \quad (53) \\
 S_F &= q_n^3(b_{12}^*M_2 - d_{11}^*) + (q_n/4)[d_{12}^* + 4d_{66}^* - \\
 &\quad M_2(b_{11}^* - 2b_{66}^*)]n^2 \\
 S_G &= p_n^2(b_{12}^*M_1 - d_{11}^*) + (n^2/4)(d_{12}^* - b_{11}^*M_1) \\
 S_H &= q_n^2(b_{12}^*M_2 - d_{11}^*) + (n^2/4)(d_{12}^* - b_{11}^*M_2)
 \end{aligned}$$

The D_n 's are the Fourier coefficients of the expansion of the right-hand side of Eq. (47) which will be denoted by K . Hence,

$$D_n = \int_0^\pi K \sin\left(\frac{ny}{a^*}\right) dy / \left[\int_0^\pi \sin^2\left(\frac{ny}{a^*}\right) dy \right] \quad (54)$$

In the same manner, the third and subsequent systems of equations may be solved. The boundary conditions depend on the solution of the previous system.

After a sufficient number of systems have been solved, the solution to the complete problem must be reconstituted by summing the solutions of the individual systems and returning to the original parameters by means of Eqs. (8, 9, 13, and 14).

Discussion

A perturbation method of solution has been applied to laminated anisotropic shells. By this scheme the effect of general anisotropy was reduced to orthotropy such that the solution to an anisotropic shell problem consists of a series of orthotropic shell solutions. The method was demon-

strated for the uniform pressurization of laminated cylindrical shells. Although the method of solution is straightforward, the amount of algebra involved is quite extensive. Therefore, it is suggested that this method be used on shell structures where the general anisotropy is slight. Then a good approximate solution may be obtained by solving a small number of systems of equations.

By letting the radius of curvature a tend to infinity throughout the equations for cylindrical shells, a system of laminated anisotropic plate equations is obtained. Techniques employed previously for cylindrical shells are again applicable for laminated anisotropic plates.

References

- 1 Dong, S. B., Pister, K. S., and Taylor, R. L., "On the theory of laminated anisotropic shells and plates," *J. Aerospace Sci.* 29, 969-975 (1962).
- 2 Ambartsumyan, S. A., *Theory of Anisotropic Shells* (Gostekhizdat Izd., State Technical Press, Moscow, 1961), Chap. 2 (in Russian).
- 3 Dong, S. B., "Mechanics of anisotropic media," Ph.D. Dissertation, Univ. Calif., Berkeley, Calif. (June 1962).
- 4 Dong, S. B., "Bending of laminated anisotropic shells," *Proceedings of the World Conference on Shell Structures, San Francisco* (October 1962).
- 5 Reissner, E. and Stavsky, Y., "Bending and stretching of certain types of heterogeneous aeolotropic elastic plates," *J. Appl. Mech.* 28, 402-408 (1961).
- 6 Vinson, J. R. and Brull, M. A., "New techniques of solution for problems in the theory of orthotropic plates," *4th U. S. National Congress of Applied Mechanics* (1962) pp. 817-826.
- 7 Novozhilov, V. V., *The Theory of Thin Shells* (P. Noordhoff Ltd., Groningen, The Netherlands, 1959) (transl. from Russian).
- 8 Dong, R. G. and Dong, S. B., "Analysis of slightly anisotropic shells," Tech. Paper 121 SRP, Aerojet-General Corp. (November 1962).

A Transient Axisymmetric Thermoelastic Problem for the Hollow Sphere

WILLIAM E. WARREN*

Sandia Laboratory, Albuquerque, N. Mex.

The linear uncoupled quasi-static theory of thermoelasticity has been applied to the elastic hollow sphere having a prescribed axisymmetric transient heat input on the outside surface, and a prescribed axisymmetric transient temperature distribution on the inside surface. Series expressions for the temperature, stress, and displacement fields are obtained in terms of orthogonal functions. As a particular example of the analysis, the stresses due to aerodynamic heating of a hypersonic hollow sphere are investigated in detail, and some representative transient and steady-state stress distributions are presented in graphical and tabular form.

Introduction

THE thermoelastic problem for a sphere has been the object of numerous investigations in the past, and bibliographies of this work may be found in the references.¹⁻³

Received April 19, 1963; revision received August 5, 1963. This work was performed under the auspices of the U. S. Atomic Energy Commission. The author is indebted to Carl B. Bailey of the Sandia Corporation Mathematical Research Department for programming the computations on the CDC 1604.

* Staff Member, Physical Sciences Research Department. Member AIAA.

Of particular interest to the present investigation is the work of Trostel,⁴ who obtains quite general solutions for general transient axisymmetric boundary conditions on the hollow sphere. The corresponding steady-state problem has been solved by McDowell and Sternberg,⁵ and a solution for the transient thermal stresses in a solid sphere has been obtained by Melan.⁶ The purpose of the present investigation is to present a detailed analysis of the transient thermal stresses in a hollow sphere subject to a prescribed axisymmetric transient heat input on the outside surface, and to a prescribed axisymmetric transient temperature distribution on the inside surface. The inner and outer surfaces are assumed

stress-free. These thermal boundary conditions may closely approximate conditions encountered during aerodynamic heating.

The analysis assumes an isotropic, homogeneous material and uses the linear uncoupled quasi-static theory of thermoelasticity. A general solution for the stress and displacement fields is obtained for the transient thermal boundary conditions as just prescribed in terms of orthogonal functions.

A particular example corresponding to aerodynamic heating of a hypersonic vehicle with a hemispherical or spherical capped nose is considered in detail, and numerical values for the maximum stresses are presented in tabular and graphical form. A second-order approximation for thin sections is also obtained for this particular example and compared with the exact results. It is found that, for thick sections where the ratio of inner radius to outer radius k is less than 0.5, the maximum stresses occur at points 90° from the nose, or stagnation point. For thinner sections with a ratio greater than 0.6, the maximum stresses occur at the nose. The particular ratio at which this change occurs is identical for the maximum tensile and compressive stresses and depends upon Poisson's ratio. For a Poisson's ratio of 0.3, the position of the maximum stress shifts at a value of $k = 0.544$. Thus, in relatively thick sections, the stresses increase, moving away from the nose, and failure will probably occur at some point remote from the nose. In thin sections the stresses decrease, moving away from the nose, and failure will probably occur at the nose. At all times, as expected, the maximum tensile stress occurs at the inside radius, and the maximum compressive stress occurs at the outside radius. For the particular time-dependent inputs considered, a steady state is reached which permits verification of the convergence of the transient series results. The solution, however, is directly applicable to the more interesting cases in which the heat input does not take on a steady-state value.

Basic Equations

In rectangular coordinates x_1' and time t' , the Cartesian tensor form of the field equations associated with the linear uncoupled quasi-static theory of thermoelasticity are†

$$\begin{aligned} \kappa T_{,ii} &= \partial T / \partial t' \\ (1 - 2\nu)v_{i',kk} + v_{k',ki} &= 2(1 + \nu)\alpha T_{,i} \\ \sigma_{ij} &= G \left[v_{i',j} + v_{j',i} + \frac{2\nu}{1 - 2\nu} v_{k',k} \delta_{ij} - \frac{2(1 + \nu)}{1 - 2\nu} \alpha T \delta_{ij} \right] \end{aligned} \quad (1)$$

In Eqs. (1), T is the temperature variation relative to some ambient temperature; v_i' and σ_{ij} represent Cartesian components of displacement and stress, respectively; δ_{ij} is the Kronecker delta; and κ, α, ν, G are material constants representing thermal diffusivity, coefficient of thermal expansion, Poisson's ratio, and shear modulus, respectively.

Introducing spherical coordinates ρ, θ, ϕ , as given by the transformation

$$\begin{aligned} x_1' &= \rho \sin\theta \cos\phi & x_2' &= \rho \sin\theta \sin\phi \\ x_3' &= \rho \cos\theta \end{aligned} \quad (2)$$

Eqs. (1) are to be solved in the region lying between the two radii $\rho = R_i$ and $\rho = R_o$, $R_i < R_o$, and subject to the following boundary conditions: a) prescribed heat input $Q(\theta, t')$ on outer radius $\rho = R_o$; b) prescribed temperature $T_i(\theta, t')$ on inner radius $\rho = R_i$; c) initial temperature $T(\rho, \theta, 0) = 0$; and d) traction free surfaces at $\rho = R_i$, $\rho = R_o$.

With the introduction of the dimensionless ratios

$$\begin{aligned} x_i &= \frac{x_i'}{R_o} & v_i &= \frac{v_i'}{R_o} & r &= \frac{\rho}{R_o} \\ t &= \frac{\kappa}{R_o^2} t' & k &= \frac{R_i}{R_o} \end{aligned}$$

† For a derivation of Eqs. (1), see, e.g., Ref. 1, Chap. 3.

Eqs. (1) become

$$T_{,ii} = \partial T / \partial t \quad (3)$$

$$(1 - 2\nu)v_{i,kk} + v_{k,ki} = 2(1 + \nu)\alpha T_{,i} \quad (4)$$

$$\sigma_{ij} = G \left[v_{i,j} + v_{j,i} + \frac{2\nu}{1 - 2\nu} v_{k,k} \delta_{ij} - \frac{2(1 + \nu)}{(1 - 2\nu)} \alpha T \delta_{ij} \right] \quad (5)$$

with the associated transformed boundary conditions

$$\left. \frac{\partial T}{\partial r} \right|_{r=1} = \frac{R_o Q(\theta, t)}{K} = q(\theta, t) \quad (6a)$$

$$T|_{r=k} = T_i(\theta, t) = h(\theta, t) \quad (6b)$$

$$T|_{t=0} = 0 \quad (6c)$$

$$\sigma_{rr}|_{r=1,k} = \sigma_{r\theta}|_{r=1,k} = \sigma_{r\phi}|_{r=1,k} = 0 \quad (6d)$$

where K is the material thermal conductivity.

The analysis proceeds with a solution of the heat equation (3) subject to (6a–6c), which gives the temperature distribution in the hollow sphere. With the temperature distribution known, a solution to the displacement equation (4) is obtained as the sum of a particular integral plus the general solution to the homogeneous form of (4) as given by the potentials of Boussinesq and Papkovich. The Boussinesq-Papkovich potentials are evaluated with the aid of (5) from the boundary condition (6d). In all that follows, the axisymmetric nature of the problem will be implicit.

Solution of the Heat Equation

The heat equation is solved by considering first the problem of time-independent boundary conditions and then applying Duhamel's theorem to obtain the solution for the more general time-dependent boundary conditions. In spherical polar coordinates, the heat equation (3) becomes

$$\frac{1}{r^2} \frac{\partial}{\partial r} \left(r^2 \frac{\partial T}{\partial r} \right) + \frac{1}{r^2 \sin\theta} \frac{\partial}{\partial \theta} \left(\sin\theta \frac{\partial T}{\partial \theta} \right) = \frac{\partial T}{\partial t} \quad (7)$$

with time-independent boundary conditions and initial condition

$$\begin{aligned} \left. \frac{\partial T}{\partial r} \right|_{r=1} &= q(\theta) & t > 0 \\ T|_{r=k} &= h(\theta) & t > 0 \\ T(r, \theta)|_{t=0} &= 0 \end{aligned} \quad (8)$$

Writing T as the sum of a steady-state solution T_s and a transient solution T_t , a separation of variables gives T_s and T_t in the form

$$T_s = \sum_{n=0}^{\infty} [\bar{A}_n r^n + \bar{B}_n r^{-n-1}] P_n(u) \quad (9)$$

$$T_t = \sum_{n=0}^{\infty} \left\{ \sum_{\alpha} [A_{n,\alpha} j_n(\alpha r) + B_{n,\alpha} n_n(\alpha r)] e^{-\alpha^2 t} \right\} P_n(u) \quad (10)$$

In Eqs. (9) and (10), $u = \cos\theta$; $P_n(u)$ is the Legendre polynomial of order n and argument u ; $\bar{A}_n, \bar{B}_n, A_{n,\alpha}, B_{n,\alpha}, \alpha$ are constants to be determined from the boundary conditions; and $j_n(\alpha r), n_n(\alpha r)$ are spherical Bessel functions‡ of the first and second kind, respectively, of order n and argument αr .

Expanding $q(u)$ and $h(u)$ from (8) in a series of the orthogonal Legendre polynomials in the form

$$q(u) = \sum_{n=0}^{\infty} q_n P_n(u) \quad h(u) = \sum_{n=0}^{\infty} h_n P_n(u) \quad (11)$$

gives the steady-state temperature in the hollow sphere as

‡ For properties of these functions, see Ref. 9, Part II, p. 1573

$$T_s = \sum_{n=0}^{\infty} \times \left\{ \frac{h_n(k/r)^{n+1}[n + (n+1)r^{2n+1}] + q_n r^n[1 - (k/r)^{2n+1}]}{[n + (n+1)k^{2n+1}]} \right\} P_n(u) \quad (12)$$

To satisfy the homogeneous boundary conditions imposed on T_t , introduce a linear combination of $j_n(\alpha r)$, $n_n(\alpha r)$ in the form

$$U_n(\alpha r) = j_n(\alpha k) n_n(\alpha r) - n_n(\alpha k) j_n(\alpha r) \quad (13)$$

and determine the admissible α 's from the condition

$$U_n'(\alpha) = 0 \quad (14)$$

The $U_n(\alpha r)$ defined by (13) and subject to (14) satisfy the required homogeneous boundary conditions imposed on T_t at $r = k$ and $r = 1$. Designating the successive zeros of $U_n'(\alpha)$ by $\alpha_{i,n}$, T_t becomes

$$T_t = \sum_{n=0}^{\infty} \sum_{i=1}^{\infty} C_{i,n} U_n(\alpha_{i,n} r) P_n(u) e^{-\alpha_{i,n}^2 t} \quad (15)$$

It may be shown from the defining differential equation and the given boundary conditions that the $U_n(\alpha_{i,n} r)$ form an orthogonal set over i in the interval $k \leq r \leq 1$ such that

$$\int_k^1 U_n(\alpha_{i,n} r) U_n(\alpha_{j,n} r) r^2 dr = \begin{cases} 0 & i \neq j \\ K_{i,n} & i = j \end{cases} \quad (16)$$

where

$$K_{i,n} = \frac{1}{2} \left\{ \frac{[\alpha_{i,n}^2 - n(n+1)]}{(n+1)^2} V_n^2(\alpha_{i,n}) - \frac{1}{\alpha_{i,n}^4 k} \right\} \quad (17)$$

and

$$V_n(\alpha_{i,n} r) = j_n(\alpha_{i,n} k) n_{n-1}(\alpha_{i,n} r) - n_n(\alpha_{i,n} k) j_{n-1}(\alpha_{i,n} r) \quad (18)$$

Substituting (12) and (15) into the initial condition (8) and making use of the orthogonality relationship (16) gives

$$C_{i,n} = \frac{-1}{\alpha_{i,n} K_{i,n}} \left[\frac{h_n}{\alpha_{i,n}^2} + \frac{q_n}{(n+1)} V_n(\alpha_{i,n}) \right] \quad (19)$$

where use has been made of the following identities readily established from (14):

$$i_n(\alpha_{i,n} k) n_{n+1}(\alpha_{i,n}) - n_n(\alpha_{i,n} k) j_{n+1}(\alpha_{i,n}) = \frac{n}{(n+1)} [j_n(\alpha_{i,n} k) n_{n-1}(\alpha_{i,n}) - n_n(\alpha_{i,n} k) j_{n-1}(\alpha_{i,n})] \quad (20)$$

$$(n+1) U_n(\alpha_{i,n}) = \alpha_{i,n} V_n(\alpha_{i,n}) \quad (21)$$

Equations (12) and (15), with (19), give the temperature in the hollow sphere as

$T =$

$$\sum_{n=0}^{\infty} \left\{ \frac{h_n(k/r)^{n+1}[n + (n+1)r^{2n+1}] + q_n r^n[1 - (k/r)^{2n+1}]}{[n + (n+1)k^{2n+1}]} - \sum_{i=1}^{\infty} \left[\frac{h_n}{\alpha_{i,n}^2} + \frac{q_n}{(n+1)} V_n(\alpha_{i,n}) \right] \frac{e^{-\alpha_{i,n}^2 t} U_n(\alpha_{i,n} r)}{\alpha_{i,n} K_{i,n}} \right\} P_n(u) \quad (22)$$

For the more general case where h_n and q_n are functions of time, that is $h_n = h_n(t)$, $q_n = q_n(t)$, Duhamel's theorem[§] gives

$$T = \sum_{n=0}^{\infty} \sum_i \tau_{i,n}(t) \alpha_{i,n} U_n(\alpha_{i,n} r) P_n(u) \quad (23)$$

where

$$\tau_{i,n}(t) = \frac{1}{K_{i,n}} \int_0^t \left[\frac{h_n(\lambda)}{\alpha_{i,n}^2} + \frac{q_n(\lambda)}{n+1} V_n(\alpha_{i,n}) \right] e^{\alpha_{i,n}^2(\lambda-t)} d\lambda \quad (24)$$

[§] Application of Duhamel's theorem is described in Ref. 7, pp. 30-32.

Solution of the Displacement Equation

With the temperature distribution in the hollow sphere determined, as in (23), the solution of the displacement equation (4) may be written as the sum of a particular integral \mathbf{v}^* and a general solution to the associated homogeneous problem corresponding to a uniform temperature distribution throughout the body which will be designated \mathbf{v}^{**} . It may be readily verified that a particular integral is obtained by taking

$$2G\mathbf{v}^* = \nabla\Phi \quad (25)$$

and

$$\nabla^2\Phi = [(1+\nu)/(1-\nu)]2G\alpha T \quad (26)$$

To formalize the solution, set

$$\left(\frac{1+\nu}{1-\nu} \right) 2G\alpha T = \sum_{n=0}^{\infty} f_n(r,t) P_n(u) \quad (27)$$

where (23) gives $f_n(r,t)$ in the form

$$f_n(r,t) = \left(\frac{1+\nu}{1-\nu} \right) 2G\alpha \sum_i \tau_{i,n}(t) \alpha_{i,n} U_n(\alpha_{i,n} r) \quad (28)$$

The particular solution to (26) to be used here is

$$\Phi = \sum_{n=0}^{\infty} H_n(r,t) P_n(u) \quad (29)$$

where

$$H_n(r,t) = \frac{1}{2n+1} \times \left[r^n \int_k^r \xi^{1-n} f_n(\xi,t) d\xi - r^{-n-1} \int_k^r \xi^{n+2} f_n(\xi,t) d\xi \right] \quad (30)$$

The spherical components of displacement and stress arising from the particular integral and the temperature terms in (5) may be obtained directly by a transformation from the Cartesian form with the aid of (26). They are

$$\begin{aligned} 2Gv_r^* &= \sum_{n=0}^{\infty} H_n(r,t) P_n(u) \\ 2Gv_{\theta}^* &= - \sum_{n=0}^{\infty} \frac{H_n(r,t)}{r} \hat{u} P_n'(u) \\ \sigma_{rr}^* &= \sum_{n=0}^{\infty} [H_n''(r,t) - f_n(r,t)] P_n(u) \\ \sigma_{\theta\theta}^* &= \frac{1}{r^2} \sum_{n=1}^{\infty} H_n(r,t) [u P_n'(u) - n(n+1) P_n(u)] + \sum_{n=0}^{\infty} \left[\frac{H_n'(r,t)}{r} - f_n(r,t) \right] P_n(u) \\ \sigma_{\phi\phi}^* &= \sum_{n=0}^{\infty} \left[\frac{H_n'(r,t)}{r} - f_n(r,t) \right] P_n(u) - \frac{u}{r^2} \sum_{n=1}^{\infty} H_n(r,t) P_n'(u) \\ \sigma_{r\theta}^* &= \frac{1}{r^2} \sum_{n=1}^{\infty} [H_n(r,t) - r H_n'(r,t)] \hat{u} P_n'(u) \end{aligned} \quad (31)$$

where $H_n'(r,t) = (\partial/\partial r)H_n(r,t)$, and $\hat{u} = \sin\theta$.

Because of the axisymmetric nature of the problem, the shear stresses $\sigma_{r\phi}$ and $\sigma_{\theta\phi}$ are identically zero and subsequently will be ignored.

It is well known that for the axisymmetric problems of elasticity the general solution to the homogeneous form of the displacement equation (4) may be obtained in terms of two Boussinesq-Papkovich potentials given, in Cartesian tensor form, by

$$2Gv_i^{**} = \phi_{,i} + x_3 \psi_{,i} - \delta_{i3}(3 - 4\nu)\psi \quad (32)$$

where x_3 is the axis of symmetry and ϕ and ψ are harmonic scalar functions. Expressions for displacements and stresses in spherical coordinates corresponding to (32), suitable for the present problem, have been obtained by Sternberg, Eubanks, and Sadowsky,⁸ and only the results will be presented here. Accordingly, the displacement and stress fields arising from (32) are

$$\begin{aligned}
 2Gv_r^{**} &= - \sum_{-\infty}^{\infty} \frac{(n+1)}{r^{n+2}} C_n P_n(u) \\
 &\quad - \sum_{-\infty}^{\infty} \frac{(n+1)(n+4-4\nu)}{r^{n+1}} D_n P_{n+1}(u) \\
 2Gv_\theta^{**} &= - \sum_{-\infty}^{\infty} \frac{C_n}{r^{n+2}} \hat{u} P_n'(u) \\
 &\quad - \sum_{-\infty}^{\infty} \frac{(n-3+4\nu)}{r^{n+1}} D_n \hat{u} P_{n+1}'(u) \\
 \sigma_{rr}^{**} &= \sum_{n=0}^{\infty} \{n(n-1)C_{-n-1} r^{n-2} + \\
 &\quad (n+1)(n+2) C_n r^{-n-3} - (n+1) \times \\
 &\quad [(n+1)(n-2) - 2\nu] D_{-n-2} r^n + \\
 &\quad n[n(n+3) - 2\nu] D_{n-1} r^{-n-1}\} P_n(u) \\
 \sigma_{\theta\theta}^{**} &= \sum_{-\infty}^{\infty} \frac{C_n}{r^{n+3}} [P_{n+1}'(u) - (n+1)(n+2) P_n(u)] \\
 &\quad - \sum_{-\infty}^{\infty} \frac{D_n}{r^{n+2}} [(n+1)(n^2 - n + \\
 &\quad 1 - 2\nu) P_{n+1}(u) - (n-3+4\nu) P_n'(u)] \\
 \sigma_{\phi\phi}^{**} &= - \sum_{-\infty}^{\infty} \frac{C_n}{r^{n+3}} P_{n+1}'(u) \\
 &\quad - \sum_{-\infty}^{\infty} \frac{D_n}{r^{n+2}} [(1-2\nu)(n+1)(2n+1)P_{n+1}(u) + \\
 &\quad (n-3+4\nu) P_n'(u)] \\
 \sigma_{r\theta}^{**} &= \sum_{n=1}^{\infty} \{-(n-1) C_{-n-1} r^{n-2} + (n+2) C_n r^{-n-3} + \\
 &\quad (n^2 + 2n - 1 + 2\nu) D_{-n-2} r^n + \\
 &\quad (n^2 - 2 + 2\nu) D_{n-1} r^{-n-1}\} \hat{u} P_n'(u) \quad (33)
 \end{aligned}$$

In (33) use has been made of the relationship $P_n(u) = P_{-n-1}(u)$. The total stress and displacement fields are then given by the sum of (31) and (33). The traction free boundary condition (6d) takes on the form

$$\begin{aligned}
 \sigma_{rr}|_{r=1,k} &= [\sigma_{rr}^* + \sigma_{rr}^{**}]_{r=1,k} = 0 \\
 \sigma_{r\theta}|_{r=1,k} &= [\sigma_{r\theta}^* + \sigma_{r\theta}^{**}]_{r=1,k} = 0 \quad (34)
 \end{aligned}$$

Substitution of (31) and (33) into the boundary condition (34) gives the following set of simultaneous equations for determining the C_n and D_n :

$$\begin{aligned}
 n(n-1) C_{-n-1} + (n+1)(n+2) C_n - \\
 (n+1)\beta_n D_{-n-2} + n\beta_{n+2} D_{n-1} &= M_n \quad n \geq 0 \\
 n(n-1) C_{-n-1} + (n+1)(n+2) k^{-2n-1} C_n - \\
 (n+1)\beta_n k^2 D_{-n-2} + (n\beta_{n+2} k^{-2n+1}) D_{n-1} &= 0 \quad n \geq 0 \\
 -(n-1)C_{-n-1} + (n+2) C_n + \delta_{n+1} D_{-n-2} + \\
 \delta_n D_{n-1} &= N_n \quad n \geq 1 \\
 -(n-1)C_{-n-1} + (n+2) k^{-2n-1} C_n + \\
 \delta_{n+1} k^2 D_{-n-2} + \delta_n k^{-2n+1} D_{n-1} &= 0 \quad n \geq 1 \quad (35)
 \end{aligned}$$

in which

$$\delta_n = n^2 - 2 + 2\nu \quad \beta_n = (n+1)(n-2) - 2\nu$$

$$M_n = f_n(1,t) - H_n''(1,t) \quad N_n = H_n'(1,t) - H_n(1,t)$$

and use has been made of the readily established fact that $f_n(k,t) - H_n''(k,t) = 0$, $H_n(k,t) = 0$, and $H_n'(k,t) = 0$. Equations (35) constitute a consistent set for determining all C_n and D_n , with the exception of C_0 , C_{-1} , D_{-1} , which correspond to a rigid-body motion of the hollow sphere. For $n = 1$, (35) gives four equations in the three variables C_1 , D_{-2} , D_0 , which are consistent by virtue of the fact that $M_1/2 = N_1$. The C_n and D_n are presented as follows:

$$\begin{aligned}
 (n-1)\Delta_n C_{-n-1} &= M_n \{ (n+1)\delta_n k^{2n+1} (1-k^2) (\delta_{n+1} + \beta_n) + \\
 &\quad \delta_{n+1} (1-k^{2n+3}) [n\beta_{n+2} - (n+1)\delta_n] \} + \\
 (n+1)N_n \{ \beta_n (1-k^{2n+3}) [n\beta_{n+2} - (n+1)\delta_n] - \\
 &\quad n\beta_{n+2} k^{2n+1} (1-k^2) (\delta_{n+1} + \beta_n) \} \quad n \geq 2 \quad (36)
 \end{aligned}$$

$$\begin{aligned}
 (n+2)\Delta_n C_n &= k^{2n+1} M_n \{ \delta_n k^2 (1-k^{2n-1}) \times \\
 &\quad [n\delta_{n+1} - (n+1)\beta_n] + \\
 &\quad n\delta_{n+1} (1-k^2) (\delta_n + \beta_{n+2}) \} + \\
 nk^{2n+1} N_n \{ (n+1)\beta_n (1-k^2) (\delta_n + \beta_{n+2}) - \\
 &\quad \beta_{n+2} k^2 (1-k^{2n-1}) [n\delta_{n+1} - (n+1)\beta_n] \} \quad n \geq 0 \quad (37)
 \end{aligned}$$

$$\begin{aligned}
 \Delta_n D_{-n-2} &= M_n \{ (n-1-k^{2n+1}) (\delta_n + \beta_{n+2}) - \\
 &\quad (2n+1)\delta_n (1-k^{2n-1}) \} + \\
 nN_n \{ (2n+1)\beta_{n+2} (1-k^{2n-1}) - \\
 &\quad (n+1)(1-k^{2n+1}) (\delta_n + \beta_{n+2}) \} \quad n \geq 0 \quad (38)
 \end{aligned}$$

$$\begin{aligned}
 \Delta_n D_{n-1} &= -k^{2n-1} M_n \{ (2n+1)\delta_{n+1} (1-k^2) + \\
 &\quad k^2 (1-k^{2n+1}) [n\delta_{n+1} - (n+1)\beta_n] \} - \\
 (n+1)k^{2n-1} N_n \{ (2n+1)\beta_n (1-k^2) - \\
 &\quad k^2 (1-k^{2n+1}) [n\delta_{n+1} - (n+1)\beta_n] \} \quad n \geq 1 \quad (39)
 \end{aligned}$$

$$\begin{aligned}
 \Delta_n &= n(1-k^{2n+1})^2 (\delta_n + \beta_{n+2}) [n\delta_{n+1} - (n+1)\beta_n] - \\
 &\quad (2n+1) \{ \delta_n (1-k^{2n-1}) (1-k^{2n+3}) \times \\
 &\quad [n\delta_{n+1} - (n+1)\beta_n] + \\
 &\quad nk^{2n-1} (1-k^2)^2 \delta_{n+1} (\delta_n + \beta_{n+2}) \} \quad (40)
 \end{aligned}$$

The evaluation of the C_n and D_n completes the determination of the stress and displacement fields in the hollow sphere. To carry out the preceding evaluations, the following terms are necessary along with $\tau_{i,n}(t)$ and $f_n(r,t)$ as given by (24) and (28):

$$H_n(r,t) = \left(\frac{1+\nu}{1-\nu} \right) \frac{2G\alpha}{(2n+1)} \sum_i \frac{\tau_{i,n}(t)}{\alpha_{i,n}^2} \times \\
 [rnk^{-n-1} - k^nr^{-n-1} - (2n+1)\alpha_{i,n} U_n(\alpha_{i,n} r)] \quad (41)$$

$$\begin{aligned}
 H_n'(r,t) &= \left(\frac{1+\nu}{1-\nu} \right) \frac{2G\alpha}{(2n+1)} \sum_i \frac{\tau_{i,n}(t)}{\alpha_{i,n}^2 r} \times \\
 &\quad [nr^nk^{-n-1} + (n+1)k^nr^{-n-1} + \\
 &\quad (n+1)(2n+1)\alpha_{i,n} U_n(\alpha_{i,n} r) - \\
 &\quad (2n+1)\alpha_{i,n}^2 r V_n(\alpha_{i,n} r)] \quad (42)
 \end{aligned}$$

$$\begin{aligned}
 [H_n''(r,t) - f_n(r,t)] &= \left(\frac{1+\nu}{1-\nu} \right) \frac{2G\alpha}{(2n+1)} \sum_i \frac{\tau_{i,n}(t)}{\alpha_{i,n}^2 r^2} [n(n-1)r^nk^{-n-1} - \\
 &\quad (n+1)(n+2)k^nr^{-n-1} - \\
 &\quad (2n+1)(n+1)(n+2)\alpha_{i,n} U_n(\alpha_{i,n} r) + \\
 &\quad 2(2n+1)\alpha_{i,n}^2 r V_n(\alpha_{i,n} r)] \quad (43)
 \end{aligned}$$

$$\begin{aligned}
 M_n &= \left(\frac{1+\nu}{1-\nu} \right) \frac{2G\alpha}{(2n+1)} \sum_i \frac{\tau_{i,n}(t)}{\alpha_{i,n}^2} \times \\
 &\quad [n(2n+1)\alpha_{i,n}^2 V_n(\alpha_{i,n}) - n(n-1)k^{-n-1} + \\
 &\quad (n+1)(n+2)k^n] \quad (44)
 \end{aligned}$$

$$\begin{aligned}
 N_n &= \left(\frac{1+\nu}{1-\nu} \right) \frac{2G\alpha}{(2n+1)} \sum_i \frac{\tau_{i,n}(t)}{\alpha_{i,n}^2} \left[(n-1)k^{-n-1} + \right. \\
 &\quad \left. (n+2)k^n + \frac{(2n+1)}{(n+1)} \alpha_{i,n}^2 V_n(\alpha_{i,n}) \right] \quad (45)
 \end{aligned}$$

Example of Aerodynamic Heating

As an application of the preceding analyses, the thermal stresses in a hollow sphere due to aerodynamic heating at hypersonic velocity will be determined. Because the rate of heat transfer to the body in the turbulent region of flow is not well defined, the analysis is assumed applicable only in the forward portion of the sphere where the flow is laminar. The analysis thus provides an approximate solution for an unyawed hemisphere or an unyawed cone capped by a spherical segment. Lees¹⁰ has obtained analytic expressions for the local heat-transfer rates for an unyawed hemisphere at hypersonic flight speeds, and his results are closely approximated over the forward half of the sphere by

$$Q(t, u) = Q_0(t) [\gamma P_0(u) + (1 - \gamma) P_2(u)] \quad (46)$$

where $Q(t, u)$ is the local heat-transfer rate, $Q_0(t)$ is the nose stagnation point heat-transfer rate, and γ is a parameter determined by flight speed ($0.39 \leq \gamma \leq 0.52$). The form of the heat input (46) cannot be assumed physically valid over the region $\pi/2 \leq \theta \leq \pi$. The theoretical results of Lees have been verified experimentally by Bloxsom and Rhodes,¹¹ and theoretical and experimental values of the stagnation-point heat-transfer rates $Q_0(t)$ have been obtained by Ferri and Zakhay.¹² Table 1 gives values of γ for various Mach numbers, as approximated from the curves of Lees,¹⁰ so as to maintain the same total heat-transfer rate into the front portion of the sphere.

If the temperature on the inside surface is assumed uniform, the steady-state effect is to raise the temperature of the entire hollow sphere by this uniform amount, which creates no stress field. The only contribution, then, to the stress field for a uniform temperature change on the inside surface will be due to transient effects. It will be assumed here that temperature changes on the inside surface are sufficiently slow so that the stress field is independent of this

$$\begin{aligned} \sigma_{rr0} &= - \left(\frac{1 + \nu}{1 - \nu} \right) \frac{8G\alpha R_0 \gamma}{Kr^3} \sum_i \Gamma_{i,0}(t) \sin \alpha_{i,0}(1 - k) \left\{ \frac{\alpha_{i,0}k[(1 - r^3)/(1 - k^3)] + \sin \alpha_{i,0}(r - k) - \alpha_{i,0}r \cos \alpha_{i,0}(r - k)}{[\alpha_{i,0}^2(1 - k) - \sin^2 \alpha_{i,0}(1 - k)]} \right\} \\ \sigma_{\theta\theta} &= \sigma_{\phi\phi_0} = \left(\frac{1 + \nu}{1 - \nu} \right) \frac{4G\alpha R_0 \gamma}{Kr^3} \sum_i \Gamma_{i,0}(t) \sin \alpha_{i,0}(1 - k) \times \\ &\quad \left\{ \frac{\alpha_{i,0}k[(2r^3 + 1)/(1 - k^3)] + (1 - \alpha_{i,0}^2 r^2) \sin \alpha_{i,0}(r - k) - \alpha_{i,0}r \cos \alpha_{i,0}(r - k)}{[\alpha_{i,0}^2(1 - k) - \sin^2 \alpha_{i,0}(1 - k)]} \right\} \end{aligned}$$

temperature, and the temperature will then be taken, with no loss in generality, as zero. In applications where the inside surface temperature is known to be nonuniform or changing rapidly, a solution for the stress field with this known temperature distribution on the inside surface and zero heat input on the outside surface may be obtained and superimposed onto the stress fields presently to be obtained.

The boundary conditions (6a) and (6b) give

$$q(u, t) = [R_0 Q_0(t)/K] [\gamma P_0(u) + (1 - \gamma) P_2(u)] \quad (47)$$

$$h(u, t) = 0 \quad (48)$$

and the nonzero q_n, h_n of (11) are

$$q_0(t) = \frac{R_0 Q_0(t) \gamma}{K} \quad q_2(t) = \frac{R_0 Q_0(t) (1 - \gamma)}{K} \quad (49)$$

Evaluating (23) and (24) with (49) gives the temperature distribution:

$$\begin{aligned} T &= \frac{2R_0 \gamma}{Kr} \sum_i \Gamma_{i,0}(t) \times \\ &\quad \left\{ \frac{\alpha_{i,0}^2 \sin \alpha_{i,0}(1 - k) \sin \alpha_{i,0}(r - k)}{[(1 - k)\alpha_{i,0}^2 - \sin^2 \alpha_{i,0}(1 - k)]} \right\} P_0(u) + \\ &\quad \frac{6R_0(1 - \gamma)}{K} \sum_i \Gamma_{i,2}(t) \times \\ &\quad \left\{ \frac{\alpha_{i,2}^5 V_2(\alpha_{i,2}) U_2(\alpha_{i,2}r)}{[\alpha_{i,2}^4 k(\alpha_{i,2}^2 - 6) V_2^2(\alpha_{i,2}) - 9]} \right\} P_2(u) \quad (50) \end{aligned}$$

Table 1 Values of γ

Mach number	2	3	5	10	∞
γ	0.52	0.46	0.42	0.40	0.39

where

$$\begin{aligned} U_2(\alpha_{i,2}r) &= \frac{1}{\alpha_{i,2}^6 r^3 k^3} \times \\ &\quad \left\{ [9(1 + \alpha_{i,2}^2 rk) - 3\alpha_{i,2}^2(r^2 + k^2) + \alpha_{i,2}^4 r^2 k^2] \sin \alpha_{i,2}(r - k) \right\} \\ &\quad - 3\alpha_{i,2}(r - k)(3 + \alpha_{i,2}^2 rk) \cos \alpha_{i,2}(r - k) \end{aligned} \quad (51)$$

$$V_2(\alpha_{i,2}r) = \frac{1}{\alpha_{i,2}^5 r^2 k^3} \left\{ [3 + 3\alpha_{i,2}^2 kr - \alpha_{i,2}^2 k^2] \sin \alpha_{i,2}(r - k) - \right\} \quad (52)$$

$$\Gamma_{i,n}(t) = \int_0^t Q_0(\lambda) e^{\alpha_{i,n}^2(\lambda - t)} d\lambda \quad n = 0, 2 \quad (53)$$

and $\alpha_{i,0}$, $\alpha_{i,2}$ are nonzero roots of the transcendental equations:

$$\alpha_{i,0} = \tan \alpha_{i,0}(1 - k) \quad (54)$$

$$\frac{\alpha_{i,2}[\alpha_{i,2}^4 k^2 + 9(1 - k)(3 + \alpha_{i,2}^2 k) - 3\alpha_{i,2}^2(1 - k)]}{[4\alpha_{i,2}^4 k^2 - 3\alpha_{i,2}^4 k - 12\alpha_{i,2}^2 - 9\alpha_{i,2}^2 k^2 + 27(1 + \alpha_{i,2}^2 k)]} = \tan \alpha_{i,2}(1 - k) \quad (55)$$

Table 2 gives the first six $\alpha_{i,0}$, $\alpha_{i,2}$ to four decimal places for three values of k .

The stress field arising from the boundary heat input $q_0(t)$ is independent of the argument u and may be obtained from (31) and (33) with the use of C_0 , D_{-2} , $f_0(r, t)$, $H_0(r, t)$, $H_0'(r, t)$, $[H_0''(r, t) - f_0(r, t)]$, and M_0 . Evaluating these terms from Eqs. (28, 37, 38, and 41-44) with the aid of (24, 40, 49, and 53) gives

$$\sigma_{\theta\theta} = 0 \quad (56)$$

where the subscript zero designates stresses from $q_0(t)$. The stresses (56) are in agreement with the results obtained by Boley and Weiner [Ref. 1, p. 301, Eq. (9.14.4)] for the symmetric thermal stresses in a hollow sphere.

The stress field arising from $q_2(t)$ is obtained from (31) and (33) in the form

$$\begin{aligned} \sigma_{rr2} &= \left\{ 2C_{-3} + \frac{12}{r^5} C_2 + 6\pi r^2 D_{-4} + \right. \\ &\quad \left. \frac{4(5 - \nu)}{r^3} D_1 + H_2''(r, t) - f_2(r, t) \right\} P_2(u) \end{aligned}$$

Table 2 Values of the first six $\alpha_{i,0}$, $\alpha_{i,2}$ for three values of k

k	0.25	0.5	0.75
$\alpha_{1,0}$	1.1263	2.3311	5.5730
$\alpha_{2,0}$	6.0653	9.2084	18.6351
$\alpha_{3,0}$	10.3435	15.5798	31.2881
$\alpha_{4,0}$	14.5694	21.8999	43.8912
$\alpha_{5,0}$	18.7786	28.2034	56.4779
$\alpha_{6,0}$	22.9804	34.4996	69.0571
$\alpha_{1,2}$	3.3579	3.7176	6.1711
$\alpha_{2,2}$	7.5235	9.8165	18.8461
$\alpha_{3,2}$	11.3753	15.9555	31.4152
$\alpha_{4,2}$	15.3463	22.1705	43.9820
$\alpha_{5,2}$	19.3960	28.4146	56.5485
$\alpha_{6,2}$	23.4909	34.6726	69.1150

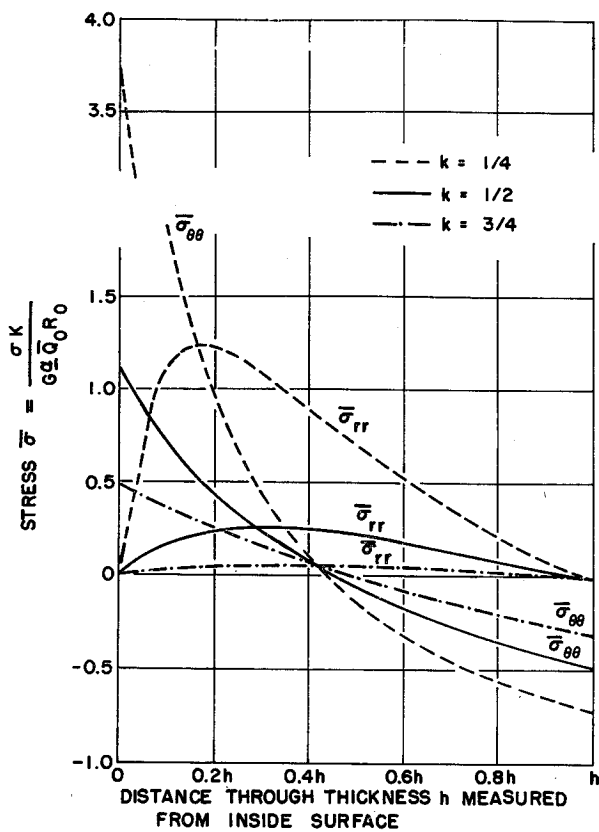


Fig. 1 Steady-state stress distribution through thickness h for $\theta = 0$, $\nu = 0.3$, $\gamma = 0.4$.

$$\sigma_{r\theta_2} = \left\{ -C_{-3} + \frac{4}{r^5} C_2 + (7 + 2\nu)r^2 D_{-4} + 2 \frac{(1 + \nu)}{r^3} D_1 + \frac{H_2(r, t) - rH_2'(r, t)}{r^2} \right\} \bar{u}P_2'(u)$$

$$\begin{aligned} \sigma_{\theta\theta_2} = \frac{3}{r^2} H_2(r, t)(1 - 2u^2) + & \left[\frac{1}{r} H_2'(r, t) - f_2(r, t) \right] \frac{(3u^2 - 1)}{2} + \\ & C_{-3}(2 - 3u^2) + \frac{3}{2} \frac{C_2}{r^5} (3 - 7u^2) - \frac{D_1}{r^3} (1 - 2\nu)(1 + 3u^2) + \\ & 3D_{-4}r^2[7(2 + \nu)u^2 - (7 + \nu)] \end{aligned}$$

$$\begin{aligned} \sigma_{\phi\phi_2} = -\frac{3}{r^2} H_2(r, t)u^2 + & \left[\frac{1}{r} H_2'(r, t) - f_2(r, t) \right] \frac{(3u^2 - 1)}{2} - \\ & C_{-3} + \frac{3}{2} \frac{C_2}{r^5} (1 - 5u^2) - \frac{D_1}{r^3} (1 - 2\nu)(9u^2 - 5) + \\ & 3D_{-4}r^2[(7 + 11\nu)u^2 - 5\nu] \end{aligned} \quad (57)$$

where the subscript 2 represents stresses arising from $q_2(t)$. The stresses in (57) may be explicitly represented with the use of (28 and 36-45) but will not be presented here.

In order to obtain numerical results, the stagnation point heat input $Q_0(t)$ was assumed to increase linearly from zero to a maximum \bar{Q}_0 and remain constant at \bar{Q}_0 thereafter. While being representative of a particular physical situation of interest, this form of heat input also has the advantage of producing a steady-state solution from which convergence of the series solution may be investigated. The steady-state solution may be obtained by using the temperature distribution (12) rather than (23) in the solution of the displacement equation with the nonzero q_n and h_n still given by (49).

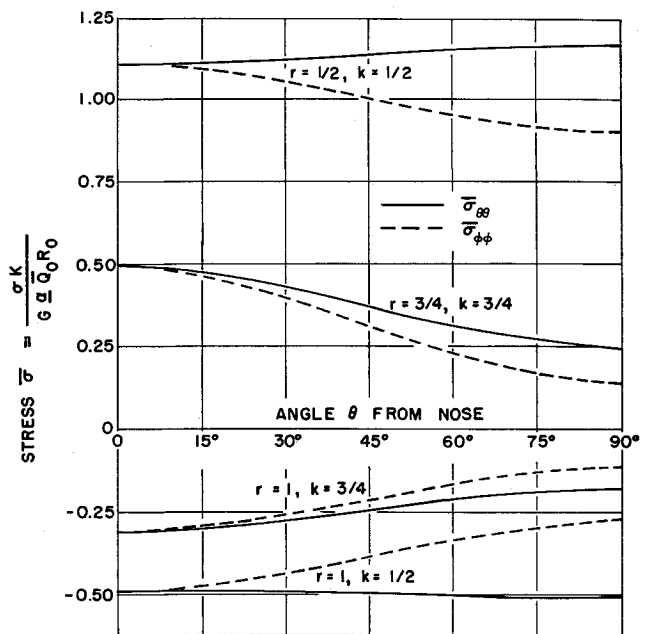


Fig. 2 Steady-state $\bar{\sigma}_{\theta\theta}$ and $\bar{\sigma}_{\phi\phi}$ at $r = 1$ and $r = k$ for $k = \frac{1}{2}, \frac{3}{4}$ and $\nu = 0.3$, $\gamma = 0.4$.

Writing

$$Q_0(t) = \begin{cases} mt\bar{Q}_0 & 0 \leq t \leq \frac{1}{m} \\ \bar{Q}_0 & t > \frac{1}{m} \end{cases} \quad (58)$$

the integral occurring in (53) is readily evaluated and found to be

$$\Gamma_{i,n}(t) = \bar{Q}_0 \begin{cases} \frac{m}{\alpha_{i,n}^4} [\alpha_{i,n}^2 t - 1 + e^{-\alpha_{i,n}^2 t}] & 0 \leq t \leq \frac{1}{m} \\ \frac{m}{\alpha_{i,n}^4} (1 - e^{\alpha_{i,n}^2/m}) e^{-\alpha_{i,n}^2 t} + \frac{1}{\alpha_{i,n}^2} & t \geq \frac{1}{m} \end{cases} \quad (59)$$

in which n is taken as 0 or 2.

The stresses (56) and (57) have been evaluated on a CDC 1604 computer for a Poisson's ratio $\nu = 0.3$, $k = 0.25, 0.5, 0.75$, and for $m = \frac{1}{2}, 1, 2, 5, 10$, and 100. Ten terms in the series expression for the stresses (56) were carried which, in the steady state, gave an error of less than 3.8% on the outside surface and negligible (less than $0.25 \times 10^{-2}\%$) error on the inside surface. The difference in error between the inside and outside boundary stresses arises because the slowly convergent terms in the series vanish on the inside radius by

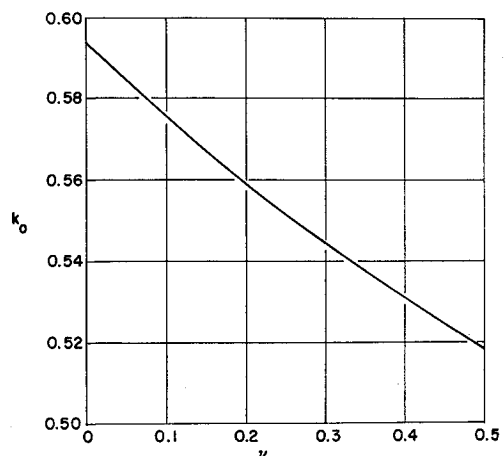


Fig. 3 Variation of k_0 with Poisson's ratio ν .

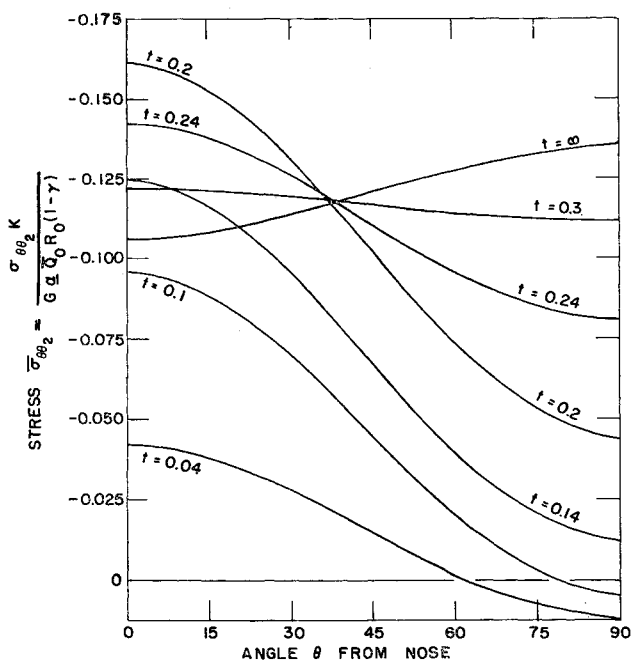


Fig. 4 $\hat{\sigma}_{\theta\theta_0}$ at $r = 1$, $k = \frac{1}{2}$, $\nu = 0.3$, $m = 0.5$ for various times t .

virtue of the form of the temperature expression and of the particular solution $\Phi(r, u, t)$ used. Ten terms in the series expressions for the stresses (57) were found to give negligible error on the inside surface in the steady state, but at other radii the nonzero, slowly convergent terms gave up to 35% error in $\sigma_{\theta\theta}$ and $\sigma_{\phi\phi}$. It was found necessary to carry 100 terms in $f_2(r, t)$ in order to reduce the error in $\sigma_{\theta\theta}$ and $\sigma_{\phi\phi}$ on the outside radius to less than 4.3%.

Some representative steady-state distributions are shown in Figs. 1 and 2. In all cases, the maximum tensile stress $\sigma_{\theta\theta}$ occurred on the inside surface $r = k$ and was found to be numerically greater than the maximum compressive stress that occurred on the outside surface $r = 1$. For k greater than 0.6, these maximum stresses occur at the nose or forward stagnation point $\theta = 0$, whereas for k less than 0.5, they occur at the equator or $\theta = \pi/2$. The value of k_0 at which the maximum stress shifts from the equator to the nose is identical for tension and compression and depends on Poisson's ratio ν , as illustrated in Fig. 3. For the two cases $k = \frac{1}{4}$ and $k = \frac{1}{2}$

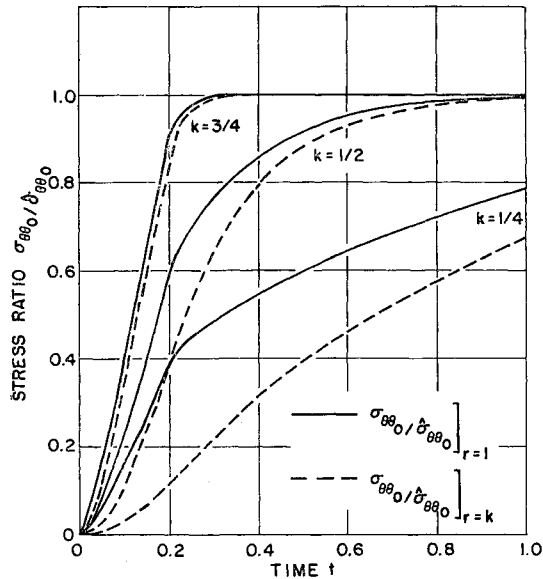


Fig. 5 Transient $\sigma_{\theta\theta_0}$ stress at $r = 1$ and $r = k$ for $m = 5$, $\nu = 0.3$, $\theta = 0$; $\hat{\sigma}_{\theta\theta_0}$ designates steady-state value.

Table 3 Components of steady-state $\hat{\sigma}_{\theta\theta}$ stress on inside and outside surface; $\theta = 0$, $\nu = 0.3$

K	$\frac{\hat{\sigma}_{\theta\theta_0} K}{G \alpha Q_0 R_0 \gamma}$ (10 terms)	$\frac{\hat{\sigma}_{\theta\theta_2} K}{G \alpha Q_0 R_0 \gamma}$ (100 terms)
Inside surface		
$\frac{1}{4}$	9.550 (9.551)	-0.187 (-0.187)
$\frac{1}{2}$	2.653 (2.653)	0.075 (0.075)
$\frac{3}{4}$	0.736 (0.736)	0.327 (0.327)
Outside surface		
$\frac{1}{4}$	-1.592 (-1.536)	-0.140 (-0.134)
$\frac{1}{2}$	-1.061 (-1.029)	-0.110 (-0.106)
$\frac{3}{4}$	-0.502 (-0.483)	-0.185 (-0.184)

investigated in detail for which $k < k_0$, this increase in the stresses from $\theta = 0$ to $\theta = \pi/2$ is at all times less than 6% of the stress at $\theta = 0$. During the transient heating, the tensile stress on the inside surface is maximum at $\theta = \pi/2$. The compressive stress on the outside surface, however, is a maximum at $\theta = 0$ during the initial heating and changes to $\theta = \pi/2$ at a later time. This effect occurs for all heat rates investigated, and a typical variation is shown in Fig. 4 for the θ -dependent part ($\sigma_{\theta\theta_2}$) of the $\sigma_{\theta\theta}$ stress.

The steady-state components of the maximum stresses on inside and outside surface at $\theta = 0$ are presented in Table 3, and the normalized transient values for $m = 5$ are shown in Figs. 5 and 6. Numbers in parentheses in Table 3 are series solutions for the number of terms indicated. It is observed from Fig. 5 that the $\sigma_{\theta\theta_0}$ stress on both inside and outside surfaces lags the instantaneous steady-state value, and the effect of increasing m is to increase the lag. The maximum stresses occur in the steady state for this particular input. This same effect is observed in Fig. 6 for $\sigma_{\theta\theta_2}$ on the inside surface, and on the outside surface for $k = \frac{3}{4}$. The $\sigma_{\theta\theta_2}$ on the outside surface for $k = \frac{1}{4}$ and $\frac{1}{2}$, however, leads the instantaneous steady-state value and exhibits an overshoot. This effect is also observed at $\theta = 0$ in Fig. 4. The magnitude of this overshoot depends on m and reaches its maximum at a time $t \geq 1/m$. An upper bound may be obtained for the ratio of the maximum overshoot to the steady-state value and for the two cases investigated; an upper

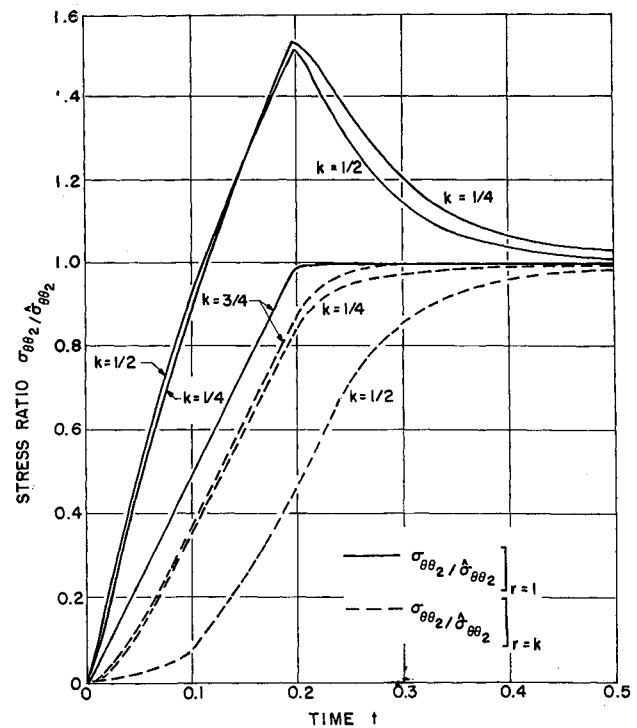


Fig. 6 Transient $\sigma_{\theta\theta_2}$ stress at $r = 1$ and $r = k$ for $m = 5$, $\nu = 0.3$, $\theta = 0$; $\hat{\sigma}_{\theta\theta_2}$ designates steady-state value.

bound is 2.02 for $k = \frac{1}{4}$, and 2.17 for $k = \frac{1}{2}$. However, for the range of γ under construction and for the given transient input, the total stress $\sigma_{\theta\theta} = \sigma_{\theta\theta1} + \sigma_{\theta\theta2}$ at no time exceeds its instantaneous steady-state value.

The curves for $k = \frac{1}{4}$ in Figs. 5 and 6 also give an indication of the error involved in neglecting transient effects and assuming instantaneous steady-state conditions for relatively thick "thin sections."

Simple expressions may be obtained for the maximum compressive and tensile stresses in thin sections. Designating h as a dimensionless thickness, i.e.,

$$h = 1 - k \quad (60)$$

and maintaining terms to order h^2 , the transient terms for a continuous $Q_0(t)$ are of order h^3 or greater and negligible. The maximum tensile stress at $\theta = 0, r = k$, as evaluated from the corresponding steady-state solution of (56) and (57), is then given by

$$\sigma_{\theta\theta}|_{r=k} = \left(\frac{1+\nu}{1-\nu} \right) \frac{G' \alpha R_0 h Q_0(t)}{K} [1 + (\gamma + \frac{2}{3})h] \quad (61)$$

and the maximum compressive stress at $\theta = 0, r = 1$ is given by

$$\sigma_{\theta\theta}|_{r=1} = - \left(\frac{1+\nu}{1-\nu} \right) \frac{G \alpha R_0 h Q_0(t)}{K} [1 - (\frac{5}{3} - 2\gamma)h] \quad (62)$$

With $h = 0.1$ ($k = 0.9$), the error in (61) and (62) is less than 3.5% in the steady state for all γ .

As previously stated, the form of the heat input over the back surface of the sphere cannot be considered physically valid, and the preceding analysis is restricted to an area around the nose. The boundary conditions (47) and (48) present an insulated surface at the equatorial plane $z = 0$, whereas in actual fact some heat transfer can be expected to take place across this plane from the forward portion of the hollow sphere to the rear portion. Also, in applications

to hemispherically capped cylinders and cones capped by a spherical segment, localized discontinuity stresses may be present at the junction of the cap and cylinder or cone. The preceding results, however, should be quite representative of the actual stresses in the aerodynamically heated thick-walled sphere or hemisphere in the region $0 \leq \theta \leq \pi/3$.

References

- Boley, B. A. and Weiner, J. H., *Theory of Thermal Stresses* (John Wiley and Sons Inc., New York, 1960), Chap. IX, p. 304.
- Parkus, H., *Instationäre Wärmespannungen* (Springer, Vienna, Austria, 1959), Chap. II, p. 64.
- Timoshenko, S. and Goodier, J. N., *Theory of Elasticity* (McGraw-Hill Book Co. Inc., New York, 1951), 2nd ed., Chap. XIV, pp. 416-421.
- Trostel, R., "Instationäre Wärmespannungen in einer Hohlkugel," *Ingr.-Arch.* 24, 373-391 (1956).
- McDowell, E. L. and Sternberg, E., "Axisymmetric thermal stresses in a spherical shell of arbitrary thickness," *J. Appl. Mech.* 24, 376-380 (1957).
- Melan, E., "Wärmespannungen bei der Abkühlung einer Kugel," *Acta Phys. Austriaca* 10, 81-86 (1956).
- Carslaw, H. S. and Jaeger, J. C., *Conduction of Heat in Solids* (Clarendon Press, Oxford, 1959), 2nd ed., Chap. I, pp. 30-32.
- Sternberg, E., Eubanks, R. A., and Sadowsky, M. A., "On the axisymmetric problem of elasticity theory for a region bounded by two concentric spheres," *Proc. First U. S. Natl. Congr. Appl. Mech.*, 209-215 (1952).
- Morse, P. M. and Feshbach, H., *Methods of Theoretical Physics* (McGraw-Hill Book Co. Inc., New York, 1953), Part II, p. 1573.
- Lees, L., "Laminar heat transfer over blunt-nosed bodies at hypersonic flight speeds," *Jet Propulsion* 26, 259-269 (1956).
- Bloxson, D. E. and Rhodes, B. V., "Experimental effect of bluntness and gas rarefaction on drag coefficients and stagnation heat transfer on axisymmetric shapes in hypersonic flow," *J. Aerospace Sci.* 29, 1429-1432 (1962).
- Forri, A. and Zakhay, V., "Measurements of stagnation point heat transfer at low Reynolds numbers," *J. Aerospace Sci.* 29, 847-850 (1962).

NOVEMBER 1963

AIAA JOURNAL

VOL. 1, NO. 11

Buckling of Cylindrical Shells under Dynamic Loads

J. D. WOOD*

Mechanics Research, Inc., El Segundo, Calif.

AND

L. R. KOVAL†

Space Technology Laboratories Inc., Redondo Beach, Calif.

The results of an exploratory experimental and analytical program on the buckling (collapse) of thin-walled cylindrical shells under dynamic loads are presented and discussed. Loading conditions for the cylinders include dead-weight axial compression with axisymmetric transient and oscillatory hydrostatic pressures. Where possible, the experimental results are qualitatively verified by linear shell theory. Areas requiring further experimental and theoretical study are identified.

I. Introduction

IN missile and space vehicle design there is an ever-increasing number of cases in which shell structures are subjected to dynamic loads. One common loading condition for

Presented at the AIAA Launch and Space Vehicle Shell Structures Conference, Palm Springs, Calif., April 1-3, 1963; revision received September 3, 1963. This work was supported by NASA Headquarters under Contract No. NASR-56. Appreciation is expressed to M. G. Rosche of NASA Headquarters and M. V. Barton, Director of the Engineering Mechanics Laboratory, Space Technology Laboratories Inc., for their encourage-

cylindrical shells is a sustained axial compression with dynamic external lateral loads. Consequently, one might expect that a condition of structural instability resulting from lateral dynamic loading could exist for thin shells.

ment, suggestions, and assistance throughout the program, and to J. P. O'Neill, R. F. Wells, and D. A. Evensen of Space Technology Laboratories for their direction and performance of the experiments.

* Vice President; formerly Associate Manager, Dynamics Department, Engineering Mechanics Laboratory, Space Technology Laboratories Inc., Redondo Beach, Calif.

† Member of the Technical Staff.